Carbon Monoxide Modulation of Microglia-neuron Communication: Anti-neuroinflammatory and Neurotrophic Role

Nuno L. Soares
NOVA Medical School, Universidade Nova de Lisboa
Inês Paiva
NOVA Medical School, Universidade Nova de Lisboa
Joana Bravo
Instituto de Biologia Molecular e Cellular: Instituto de Biologia Molecular e Celular
Claudia S. F. Queiroga
NOVA Medical School, Universidade Nova de Lisboa
Bernadete F. Melo
NOVA Medical School, Universidade Nova de Lisboa
Silvia V. Conde
NOVA Medical School, Universidade Nova de Lisboa
Carlos C. Romão
Instituto de Tecnologia Química e Biológica
Teresa Summavielle
Universidade do Porto
Helena L.A. Vieira (hl.vieira@fct.unl.pt)
NOVA School of Science and Technology, Universidade Nova de Lisboa https://orcid.org/0000-0001-9415-3742

Research Article

Keywords: microglia, neurons, carbon monoxide, neuroinflammation, neurotrophism

Posted Date: October 12th, 2021

DOI: https://doi.org/10.21203/rs.3.rs-745011/v2

Version of Record: A version of this preprint was published at Molecular Neurobiology on November 18th, 2021. See the published version at https://doi.org/10.1007/s12035-021-02643-z.

Abstract

Microglia, the ‘resident immunocompetent cells’ of the central nervous system (CNS), are key players in innate immunity, synaptic refinement and homeostasis. Dysfunctional microglia contribute heavily to creating a toxic inflammatory milieu, a driving factor in the pathophysiology of several CNS disorders. Therefore, strategies to modulate the microglial function are required to tackle exacerbated tissue inflammation. Carbon monoxide (CO), an endogenous gaseous molecule produced by the degradation of haem, has anti-inflammatory, anti-apoptotic, pro-homeostatic and cytoprotective roles, among others.

ALF826A, a novel molybdenum-based CO-releasing molecule, was used for the assessment of neuron-microglia remote communication. Primary cultures of rat microglia and neurons, or the BV-2 microglial and CAD neuronal murine cell lines, were used to study the microglia-neuron interaction. An approach based on microglial-derived conditioned media in neuronal culture was applied. Medium derived from CO-treated microglia provided indirect neuroprotection against inflammation by limiting the lipopolysaccharide (LPS)-induced expression of reactivity markers (CD11b), the production of reactive oxygen species (ROS) and the secretion of inflammatory factors (TNF-α, nitrites). This consequently prevented neuronal cell death and maintained neuronal morphology In contrast, in the absence of inflammatory stimulus, conditioned media from CO-treated microglia improved neuronal morphological complexity, which is an indirect manner of assessing neuronal function. Likewise, the microglial medium also prevented neuronal cell death induced by pro-oxidant *tert*-Butyl hydroperoxide (*t*-BHP). ALF826 treatment reinforced microglia secretion of Interleukin-10 (IL-10) and adenosine, mediators that may protect against *t*-BHP stress in this remote communication model. Chemical inhibition of the adenosine receptors A_{2A} and A_1 reverted the CO-derived neuroprotective effect, further highlighting a role for CO in regulating neuron-microglia communication *via* purinergic signalling.

Our findings indicate that CO has a modulatory role on microglia-to-neuron communication, promoting neuroprotection in a non-cell autonomous manner. CO enhances the microglial release of neurotrophic factors and blocks exacerbated microglial inflammation. CO improvement of microglial neurotrophism under non-inflammatory conditions is here described for the first time.

Background

Microglia are the main immune cell population in the Central Nervous System (CNS) [1]. Originating from a primitive myeloid precursor [2], microglia populate the brain and spinal cord, where they account for 5-10% of total glial population with crucial biological functions [1, 3]. As the brain first line of defence, microglia are sentinels that constantly screen the brain parenchyma. When encountering potentially pathogenic or toxic agents that endanger the CNS integrity, microglia initiate an inflammatory response [1, 3]. This response involves major functional and morphological changes, namely alteration of microglia expression of surface receptors, intracellular enzymes and secreted molecules [1]. Release of inflammatory mediators, such as reactive oxygen species (ROS) [4, 5] and nitric oxide (NO) derivatives [3, 6, 7], cytokines [3, 6, 7], metabolites and extracellular vesicles [8] induce cell death on compromised

cellular populations and/or potentiate the microglial phagocytosis of bacteria, viruses and debris [1, 9, 10]. Additionally, microglia recruit other cells and help set up the adaptive immune response [11]. Conversely, microglia also have a relevant role in neurotrophic support [12], as well as brain development, removing immature and apoptotic populations [13]. Microglia also participate in the regulation of synaptic plasticity and neuronal activity [14–17], and stimulate synaptogenesis and synaptic maturation [18, 19]. Several of these functions are reliant on microglia paracrine mechanisms, through secretion of specific factors like thrombospondin, Insulin growth factor 1 (IGF-1) [12, 20–24], brain-derived neurotrophic factor (BDNF), adenosine, Interleukin-10 (IL-10) as well as low levels of inflammatory cytokines TNF-α (Tumour necrosis factor α) and IL-1β [25–28]. Being both the hub of neuroinflammation, and crucial for neuronal development, survival and activity, microglia function is under tight regulation. Deficient microglial function causes imbalances in brain tissue homeostasis: by affecting synaptic plasticity and the overall neuronal function [1] and/or by triggering exacerbated inflammation, which is a common feature of both chronic and acute CNS disorders [29, 30].

Known for its toxicity, carbon monoxide (CO) is a gaseous molecule, endogenously produced by the degradation of haem catalysed by haem oxygenase (HO) [31]. This reaction yields CO, along with free iron (Fe^{2+}) and biliverdin [31, 32]. HO has two described isoforms: the constitutive form HO-2 and HO-1, an inducible isozyme, whose expression is activated by a wide array of stress signals [32]. CO is a signalling molecule and the CO/HO-1 axis is protective in several biological contexts, modulating inflammation, apoptosis, cell differentiation and metabolism [33–35] CO-derived ROS production primes the anti-inflammatory player peroxisome proliferator-activated receptor gamma co-activator 1 α (PPAR-γ) in macrophages [36] and lung [37], decreasing downstream pro-inflammatory mediators. CO also regulates the activities of mitogen activated protein kinase (MAPK), resulting in lower secretion of key cytokines, which limits pro-inflammatory stimulation [38–40]. In CNS, CO has been described as neuroprotective by preventing neuronal cell death *in vitro* [41, 42] and in ischaemia and reperfusion *in vivo* models [43, 44]. In glial cells, CO is cytoprotective in astrocytes, namely CO inhibited apoptosis by regulating mitochondrial membrane permeabilization[45], by improving oxidative metabolism [46] and by modulating P2X7 receptors [47]. Likewise, vasodilation is promoted by CO *via* astrocytic glutamate receptors [48]. In microglia, CO reduces inflammatory response induced by LPS (lipopolysaccharide), thrombin or Interferon γ (IFN-γ) [38, 49]. This anti-inflammatory effect occurs by chemically inhibiting PI3K (Phosphoinositide 3-kinase) an ERK (Extracellular-signal-regulated kinase) [38, 49]. CO also decreases neuroinflammation in microglia *via* modulation of cell metabolism, namely by enhancing mitochondrial respiration [50]. *In vivo* models of CNS disorders have highlighted the potential of CO as a regulator of local brain immunity. In fact, CO treatment ameliorates tissue inflammation and limits cell loss and disease progression in models for autoimmune encephalomyelitis [51] and haemorrhagic stroke [52].

Herein, we aimed to assess how CO alters microglia function and paracrine communication with the surrounding cellular milieu, particularly with neurons. In fact, CO's role on microglia-neuron direct communication has not been an object of study to the best of our knowledge. Thus, the present work

targets the underlying molecular mechanisms of this intercellular communication primarily by the analysis of neuroinflammatory and neurotrophic factors in microglial secretome. Then, it is explored how secretome from CO-treated microglia affects neuronal survival, morphology and function.

The therapeutic advent for CO is supported by the increasing number of applications [32] and can be clinically implemented by the development of CO-releasing molecules (CORMs) to circumvent several limitations regarding CO's pharmacological delivery, namely safety and tissue specificity [53–55]. Herein, a novel CORM, ALF826, is used to assess the impact of CO on microglial neuroinflammation and neurotrophism, and on microglia-neuron communication. ALF826 is a molybdenum carbonyl complex which spontaneously releases CO in biological media. Moreover, molybdenum is a trace element that is essential for the function of at least three human enzymes: xanthine oxidase, sulphite oxidase and aldehyde oxidase.

Methods

Materials

All cell culture plastics were purchased from Corning (Corning, NY) and Sarstedt (Sarstedt, Germany). Chemicals of analytical grade were obtained from Sigma-Aldrich (St Louis, MI), unless stated otherwise. All used antibodies and their respective technique are described in Supplementary Table 1.

Cell line cultures

BV2 murine microglia cell line was kindly supplied by Dr Ana Raquel Santiago (Faculdade de Medicina da Universidade de Coimbra). Cells were grown in RPMI-1640 medium (Sigma-Aldrich), supplemented with 10% foetal bovine serum (FBS, Thermo-Fisher Scientific), 4 mM L-glutamine (Thermo-Fisher Scientific), penicillin (100 units/mL) and streptomycin (100 µg/mL) (Thermo-Fisher Scientific). CAD mouse catecholaminergic neuronal cell line was gently provided by Dr Federico Herrera (Faculdade de Ciências da Universidade de Lisboa). DMEM/F12 was used as basal medium (Thermo-Fisher Scientific) and supplemented with 8% FBS (Thermo-Fisher Scientific), penicillin (200 units/mL) and streptomycin (200 µg/mL) (Thermo-Fisher Scientific). For differentiation, growing medium was replaced by a serum free DMEM/F12 supplemented solution. SH-SY5Y human neuroblastoma was used. For cell maintenance, DMEM/F12 was used as basal medium (Thermo-Fisher Scientific) and supplemented with 8% FBS (Thermo-Fisher Scientific), penicillin (200 units/mL) and streptomycin (200 µg/mL) (Thermo-Fisher Scientific). All cell lines were maintained in a humified incubator at 37°C and 5% CO_2.

Primary cell cultures

Animals were housed in standard laboratory conditions with free access to water and standard rodent chow. All animal experiments were performed with the approval of the i3S Animal Ethics Committee and

in accordance with European Union Directive on the protection of animals used for scientific purposes (2010/63/EU) and the Portuguese Law that transposes it (Decreto-Lei n.º 113/2013). All efforts were made to minimize animal suffering. Neuron hippocampal cell cultures were isolated from embryonic day 18 Wistar rats. Pregnant females were euthanized in a CO_2 chamber, their abdominal region was pulverized with 70% ethanol and opened using surgical scissor and tweezers. Embryos were retrieved, decapitated and the brains were placed in a Petri dish containing Hank's Balanced Salt Solution (HBSS, Thermo-Fisher Scientific) supplemented with 100 µg/mL Gentamicin (Lonza). The brains were dissected under a magnifying glass, and the hippocampi were collected. Hippocampal tissue was incubated for 15 minutes at 37°C with 1.5 mg/mL of trypsin (Thermo-Fisher Scientific) and after allowing the hippocampi to sediment, the supernatant was removed and a 10% FBS (Thermo-Fisher Scientific) solution was added. Following gentle agitation, the supernatant was discarded, and a washing step was performed with fresh HBSS. The supernatant was again removed and Neurobasal medium (Thermo-Fisher Scientific) supplemented with 25 µM Glutamate (Sigma-Aldrich), 0.5 mM L-glutamine (Thermo-Fisher Scientific), 100 µg/mL Gentamicin (Lonza) and 1% B27 supplement (Thermo-Fisher Scientific) was added, and the tissue was dissociated by thorough pipetting. The suspension was then put through a 70µm cell strainer, collected and cells were counted with a Neubauer counting chamber. Neurons were plated on 24 multi-well plates (100 000 cells/well), on top of Poly-D-Lysine (PDL, 1 mg/mL, Sigma-Aldrich) coated glass coverslips. Cells grew *in vitro* for 10 days before any analysis was carried forward, with fresh medium being added after seven days in culture.

Mixed glial cell (MGC) cultures were obtained from cortices of 2-day old Wistar pups. Animals were quickly sacrificed, with brains being removed and dissected consequently in HBSS (Thermo-Fisher Scientific) with penicillin (100 units/mL) and streptomycin (100 µg/mL) (Thermo-Fisher Scientific). White matter and meninges were discarded, and the remaining tissue was collected and mechanically homogenized. The cell suspension was passed through a 25-gauge syringe and incubated with 0.1 U/mL DNAse I (Zymo) and 1.5 mg/mL trypsin (Thermo-Fisher Scientific) for 15 minutes at 37°C. After incubating, trypsin was inactivated by adding DMEM GlutaMAX (Thermo-Fisher Scientific) supplemented with penicillin (100 units/mL), streptomycin (100 µg/mL) (Thermo-Fisher Scientific), 10% FBS (Thermo-Fisher Scientific) and the suspension was centrifuged afterwards (550 g, 15 minutes). The resulting supernatant was carefully discarded, and the pellet was resuspended in the same medium and put through a 100 µm cell strainer. The obtained suspension was distributed equally into 75cm^2 t-flasks (2 brain per flask) to make a total media of 10mL per flask. Prior to adding the cells, the t-flasks were coated with 1 mg/mL PDL (Sigma-Aldrich) for 1 hour. The cell medium was changed every other day.

Primary microglia cells were obtained from 10-day-old MGC cultures, which were placed on an orbital shaker incubator for 2h at 200 rpm. The cell suspension was collected, centrifuged (260 rcf, 10 minutes) and the supernatant was discarded. The pellet was resuspended in DMEM/F12 (Thermo-Fisher Scientific) and cells were counted using a Neubauer counting chamber. Microglia cells were always obtained from either 10 (shake 1) or 17 days *in vitro* (DIV, shake 2) MGC cultures. Older cell cultures were not considered for this. Microglial cells were plated on 24 multi-well plates, with DMEM/F-12 GlutaMAX (Thermo-Fisher

Scientific) and 4% L-glutamine (Sigma-Aldrich), penicillin (10 units/mL) and streptomycin (10 µg/mL) (Thermo-Fisher Scientific) and 10% FBS (Thermo-Fisher Scientific) supplement.

Cell culture treatments

For neuroinflammatory assay, BV2 cells were seeded onto multi-well plates (10 x 10^4 cells *per* well), treated with ALF826 (50µM) for 24h before LPS (Lipopolysaccharide, 500 ng/mL, Sigma-Aldrich) was added for another 24h. Subsequently, the BV2 microglia conditioned media was collected and centrifuged for 5 minutes, 500g (Figure 1A). Simultaneously, CAD neurons were seeded (6 x 10^4 cells *per* well) and 24h later differentiating medium was added. After 48h of differentiation, neuronal supernatant was removed, and CAD were challenged for one day with BV2 microglia conditioned media.

For neurotrophic assay, BV2 cells (10 x 10^4cells *per* well) were treated for 48h with ALF826 (50µM), then medium was collected and centrifuged (5 minutes, 500g). The conditioned medium (microglial culture supernatant) was added into 48h-differentiated CAD neuronal culture. *t*-BHP at 7.5 and 10 µM was added into the CAD neuronal culture to promote cell death for 24h, with or without the presence of BV2 microglia conditioned medium, when mentioned (Figure 7A). To assess the effect of purinergic signalling on neuron-microglia communication, 48h-differentiated CAD neurons were treated, simultaneously, with microglia conditioned media and adenosine receptor antagonists SCH-58261 (1 and 5 µM) and Dipropylcyclopentylxanthine (DPCPX, 25 and 50 µM). Primary culture of microglia derived from 10 or 17 DIV MGC cultures was collected and plated on 24 multi-wells (7x10^5 cells/well). 24h after seeding, cells were treated with 50 µM of ALF826 for 24h then with 10 ng/mL of LPS for another 24h. Microglia medium was collected, centrifuged at 500 g for 5 min and its supernatant was used as conditioned medium. 50% volume of the neuronal medium of 10 DIV hippocampal neurons cultured in 24 multi-well plates was replaced by microglia conditioned media. Neuronal cells were analysed following 24h.

Reagents and solution preparation

ALF826 was provided by Proterris (Portugal) Lda. Stock solutions of 2.5mM were prepared by dissolving the compound in Dimethyl sulfoxide (DMSO, Sigma-Aldrich) and diluting it 1/10 in a $NaHCO_3$ solution (0.1mM, pH 8.3). ALF826 was then filtered, aliquoted and stored at -80°C at a final concentration of 2.5 mM. ALF-826 has a half-life of 37 min in Hepes 7.4 buffer. Its cytotoxicity is negligible at 100µM (98% survival of RAW246.7 macrophages at 24h) and its CO effective load is *ca*. 3 equivalents of CO per mol (Information provided by Proterris (Portugal) Lda.)

For the preparation of the depleted form of ALF826 (iALF826), the compound was dissolved in DMSO, left for 24h at room temperature to allow for the dissociation of the CO groups from the molecular scaffold and subsequently diluted in 1/10 in a $NaHCO_3$ solution (0.1mM, pH 8.3). iALF826 was then filtered, aliquoted and stored at -80°C at a final concentration of 2.5 mM.

Fresh CO gas solutions of CO were prepared by saturating PBS, bubbling 100% of CO compressed gas (Linde, Germany) for 30 minutes, yielding a 10^{-3} M stock solution. CO concentration in solution was measured spectrophotometrically, by the conversion of deoxymyoglobin to carbon monoxymyoglobin, in an assay previously described by Motterlini et al. [53].

Flow Cytometry

Neuronal cell viability assay

CAD neurons were collected by trypsinization and stained with 1ng/mL of Propidium Iodide (PI, Thermo-Fisher Scientific) for 15 minutes at 37°C. Cell viability was analysed by flow cytometry using the FACS Canto II (BD Biosciences). 488nm laser line was used for excitation, and PI was read in the FL-3 channel in the linear scale. Appropriate controls, such as positive staining controls and unstained samples were always carried out. Data analysis was performed with the FlowJo software (BD Biosciences).

Microglia reactivity assay

BV2 cells were collected by scrapping and stained with 500 ng/mL of PE/Cy7 (Phycoerythrin/Cyanine 7) anti-mouse CD11b antibody (BioLegend) for 15 minutes at 37°C. Microglia reactivity was analysed by flow cytometry using FACS Canto II (BD Biosciences). 488nm laser line was used for excitation, and reactivity levels were determined by reading sample's PE/Cy7 Median Fluorescence Intensity in the FL-4 channel in the linear scale. Appropriate controls, such as positive staining controls and unstained samples were always carried out. Subsequent data analysis was performed using FlowJo software (BD Biosciences).

Enzyme-linked immunosorbent assay

Enzyme-linked immunosorbent assay (ELISA) was performed to measure Tumour necrosis factor α (TNF-α), Interleukin-1 β (IL-1β) and IL-10 microglia supernatant levels, using the respective Standard ABTS ELISA Development Kits (PeproTech). For Glial cell-derived neurotrophic factor (GDNF) and Brain-derived neurotrophic factor (BDNF), different kits were used (GDNF ELISA Kit (Abcam), Human/Mouse BDNF DuoSet ELISA (R&D)). Microglia culture media was collected and centrifuged to remove cellular debris, and the pellet was discarded. The resulting supernatant was kept at -80°C until analysis. All experiments were performed in accordance with the respective manufacturer's instructions. Absorbance values were measured at 415nm, with wavelength correction set at 560nm, using an Infinite F200 PRO microplate reader (Tecan).

Griess reaction assay

Nitrite of microglia supernatant was quantified by Griess reaction colorimetric test. Microglia culture media was collected and centrifuged to remove cellular debris and subsequently incubated with Griess reagent (1:1 ratio, Sigma-Aldrich) for 10 minutes at room temperature (RT), protected from light. Absorbance was measured at 540 nm using an Infinite F200 PRO microplate reader (Tecan). Nitrite concentration was calculated with reference to a standard curve generated with known concentrations of sodium nitrite ($NaNO_2$, Sigma-Aldrich).

Immunoblotting

Cell extracts were washed several times with ice-cold PBS and lysed with RIPA (Radioimmunoprecipitation assay) buffer (50 mM Tris-HCl, pH 6.8, 50 mM NaCl (w/v), 0.1% SDS (w/v), 1% sodium deoxycholate (w/v), 1% Triton X-100 (v/v), 10% Glycerol (v/v), 1% protease inhibitor cocktail (v/v). Protein concentration was determined with a Pierce BCA Protein Assay Kit (Thermo-Fisher Scientific), following manufacturer's instructions. Absorbance values were registered at 560 nm using an Infinite F200 PRO microplate reader (Tecan). A Bovine Serum Albumin (BSA, Merck) standard curve was constructed to determine protein concentration.

Equal amounts of protein were separated by sodium dodecyl sulphate–polyacrylamide gel electrophoresis (SDS-PAGE) on a polyacrylamide gel (10% gel unless stated otherwise), with a NZYColour Protein Marker II (NZYtech) being used as band size reference. Proteins were then electrically transferred onto an Amersham Protran 0.45 NC nitrocellulose membrane (GE LifeSciences) and blocked with 5% (m/v) BSA in T-TBS for 1h. Membranes were labelled consecutively with primary and secondary antibodies as indicated in Supplementary Table 1. Immunoblots were exposed to ECL Clarity Western Detection Reagent (Bio-Rad) 5 minutes and the reactive bands were detected after the membranes were exposed to X-ray film (Chemidoc Touch Imaging System, Bio-Rad). The resulting area and intensity of the bands were quantified with ImageLab software (Bio-Rad). β-actin was used as internal loading control unless otherwise is stated.

ROS generation assay

ROS, in particular hydrogen peroxide generation, were measured following the conversion of 2', 7' -dichlorofluorescein diacetate (H2DCFDA) (Invitrogen) to fluorescent 2', 7' -dichlorofluorescein (DCF). BV2 microglia cells were seeded (9 x 10^3 cell/well) on 96-well black flat bottom plates and treated with ALF826 and/or LPS, as described previously. After treatment, microglia supernatant was removed, and cells were washed twice with ice-cold PBS and treated for 15 minutes with 5 μM of H2DCFDA. Cells extracts were subsequently washed, and fluorescence intensity was measured using a Tecan Infinite F200 PRO microplate reader (λ_{ex} 485 nm/λ_{em} 530 nm). ROS generation was calculated as increase over baseline levels, determined for untreated cells and normalized to total protein quantification for each condition.

Immunofluorescence microscopy

Cells growing on glass coverslips were fixated with 4% (v/v) PFA (paraformaldehyde) and 4% (w/v) sucrose solution (20 minutes at RT), permeabilized with 0.3% (v/v) Triton X-100 solution (15 minutes, RT) and then blocked with BSA 1% (w/v) and Triton X-100 0.1% (w/v) for half hour at RT. Later, cells were probed with primary (2h incubation) and secondary (1h) antibodies, as described in Supplementary Table 1. Coverslips were mounted onto glass slides with Prolong mounting medium (with DAPI 1:1000 (4',6-diamidino-2-phenylindole, Thermo-Fisher Scientific). Washing with ice-cold PBS was always performed between steps. All antibodies used were diluted in 1%(v/v) BSA and 0,1%(v/v) Triton X-100 solution. Fixating, permeabilizing and blocking solutions were prepared in PBS. Images were captured with a Zeiss Z2 microscope, with at least five random micrographs being acquired, unless otherwise stated.

Neuronal morphology analysis

Neurite tracing was done using the NeuronJ Fiji plug-in (Erik Meijering) and following instructions present in an online manual provided by the developer (https://imagescience.org/meijering/software/neuronj/manual/). Neurites were labelled and clustered as primary (originating from cell soma), secondary (from a primary neurite) and tertiary (from a secondary neurite) processes. Software calculation determined total number of neurites per field as well as individual neurite length. Similarly, neuron skeleton reconstruction and Sholl analysis (quantification of intersections at concentric spheres originating from cell soma to 150µm, with radius every 5 µm) were performed using the Simple Neurite Tracer Fiji plug-in, in accordance to instructions present in online tutorials (https://imagej.net/Simple_Neurite_Tracer). For each individual experiment, four to six images were analysed for each glass slide.

High-performance liquid chromatography

To quantify microglial adenosine levels, supernatant from BV2 cells was collected from each well, and deproteinized in PCA 3M, centrifuged at 4ºC, 10 min, 13000 g. Then the supernatants neutralized (pH 6.8-7.2) with KOH/Tris (Sigma-Aldrich) as previously described by Conde and Monteiro (2004). Adenosine was quantified by HPLC with UV detection at 254 nm. The HPLC system consisted of an LC 10-AD pump, SIL-20AC autosampler, SPD-20 A/AV UV-VIS wavelength detector and Class VP software to analyse the chromatograms (Shimadzu, Kyoto, Japan). The analytical column was a Lichrospher 100 RP-18 (125 4 mm, i.d., particle size 5 µm, Merck, Madrid, Spain) protected by LichroCART 4–4 guard-columns (Merck, Madrid, Spain). The mobile phase was 100 mm KH2PO4 with 15% methanol, pH 6.5, run at a flux of 1.75 ml min−1. External standards were prepared under the same conditions as the biological samples and adenosine identification and quantification was made against the standards. Adenosine supernatant levels were normalized to total protein microglial content.

Statistical analysis

Results are presented as mean ± standard error of the mean (SEM), with at least three biological replicates being performed for all experiments. All statistical analysis was performed using the Prism 6.0 software (GraphPad), with the one-way ANOVA test being performed.

Results

Conditioned medium from CO-treated microglia provides neuroprotection to neuronal culture against cell death

In order to assess the role of carbon monoxide (CO) on remote neuron-microglia communication, a conditioned medium approach was used, which allows to evaluate the impact of microglia secretome on neuronal function and survival. BV2 microglia were pre-treated with 50μM ALF826 for 24h and then incubated or not with 500 ng/mL of LPS (Lipopolysaccharide), a TLR-4 (Toll-like receptor) agonist, classically used to elicit an inflammatory-like response. After one day, microglia medium was collected and added into the catecholaminergic neuronal cell line CAD culture for 24h, challenging cell survival (Figure 1A). Neuronal cell survival assessment was based on membrane integrity (Propidium iodide internalization) by flow cytometry (Figure 1B). Viability of CAD neuronal cells exposed to conditioned media derived from inflammatory microglia decreased, and this effect was partially prevented whenever BV2 microglia were pre-treated with ALF826 (Figure 1B). In addition, expression of neuronal cleaved caspase-3 (Figure 1C), which is a classical biomarker of apoptosis, was quantified by Western Blot. Accordingly, supernatant derived from CO-treated microglia also decreased the levels of cleaved caspase-3 in neurons. These data indicated that CO decreases microglia release of neurotoxic factors, limiting neuronal cell death.

The data obtained in BV2 microglia-CAD neuron conditioned media protocol were then validated in a more physiologically relevant model: hippocampal neuronal and microglia rat primary cultures. Primary cultures of microglia were treated with ALF826 (50 μM, 24h) and LPS (10 ng/mL, 24h) and the supernatant was collected, centrifuged and subsequently incubated 1:1 (volume) with neuronal media to challenge 10 days *in vitro* (DIV) hippocampal neurons. To assess neuronal cell death in primary cultures, neurons were immunolabeled with an antibody against βIII-tubulin (green), the nuclei were stained with DAPI (blue) and cells were imaged using a fluorescence microscope (Figure 1D). Apoptosis was quantified by counting chromatin condensed nuclei (Figure 1E). In accordance with data from Figure 1B, neurons cultured with inflammatory conditioned media presented a significant decrease in cell survival, which was prevented whenever microglia were pre-treated with ALF826.

Conditioned medium from CO-treated microglia improves neuronal morphology

Neuronal morphology of differentiated CAD cell line was analysed for indirect evaluation of neuronal function (Figure 2). Neurons exposed to inflammatory microglia media presented a decrease in cellular

complexity parameters, such as average neurite length (Figure 2A) and number of neurites *per* cell (Figure 2B). Additionally, data from *Sholl* analysis, which is a quantitative method used for the analysis of neuronal arborization, further indicated the existence of a decrease of the overall neuronal complexity whenever neurons were challenged with inflammatory conditioned media (Figure 2C and D). Conditioned medium derived from CO-treated microglia prevented the decrease of neurite length and the number of neurites *per* cell and maintained neurite arborization at similar levels as the non-treated control neurons. Thus, microglial ALF826 treatment has a paracrine neuroprotective effect on neuronal cells, potentially achieved through modulation of microglial release of neurotoxic pro-inflammatory factors.

CO has an anti-inflammatory role on LPS-challenged BV2 microglia

Since CO appears to provide neuroprotection by regulating neuron-microglia remote communication, we next quantified extracellular levels of the pro-inflammatory factors: nitric oxide (NO), Tumour necrosis factor α (TNF-α) and Interleukin-1β (IL-1β) in microglial supernatant, all of which promote inflammation. Griess colorimetric assay, which allows for the quantification of nitrites, an indirect measure of NO, indicated an increase in nitrites concentration following LPS exposure (Figure 3A). Thus, ALF826 treatment partially inhibited LPS-induced nitrite release. The decrease of nitrite secretion was dependent on ALF826 concentration (data not shown). TNF-α was quantified by ELISA, CO also prevented the secretion of TNF-α pro-inflammatory cytokine in LPS BV2 (Figure 3B).

To confirm that the effect of ALF826 was due to the CO release and not of the scaffold of the molecule, nitrite levels were also assessed in BV2 cells following treatment with a CO-saturated PBS solution (50 μM). In fact, the saturated solution also reverted NO secretion in LPS-stimulated microglia (Figure S1A). To further confirm the effect of the CO-releasing molecule, LPS-treated microglia were also incubated with either ALF826 or with the CO depleted form (iALF826). Here, while ALF826 inhibited secretion of NO (Figure S1B) and TNF-α (Figure S1C), iALF826 did not produce such effect.

It was next addressed whether CO anti-neuroinflammatory function is present in primary cultures of microglia. Microglial medium was collected for indirect quantification of NO levels by Griess colorimetric assay and of TNF-α and IL-1β levels by ELISA. For all three secreted factors, LPS triggered a significant increase, which were all partially prevented in the presence of ALF826 pre-treatment (Figure 3C, D and E). Contrary to BV2 cell line (data not shown), in microglial primary cultures LPS elicited elevated levels of IL-1β, suggesting a strong NLRP3 (NLR Family Pyrin Domain Containing 3) inflammasome reaction. Altogether, these results validate that CO limits exacerbated inflammation, by reducing the levels of secreted pro-inflammatory factors.

To further confirm the anti-inflammatory effect of ALF826 treatment on BV2 function, we quantified the expression of specific microglial reactivity markers: intracellular ROS production and surface receptor CD11b. The role of CO on intracellular ROS production was evaluated by H(2)DCF-DA staining that

increases its fluorescence in the presence of hydrogen peroxide. Likewise, CO partially inhibited LPS-induced microglia-derived oxidative stress (Figure 4A). Finally, expression of surface receptor CD11b was quantified *via* flow cytometry. CD11b immunoreactivity increased in LPS-administered microglia and this was partially reverted, in ALF826 pre-treated cells (Figure 4B).

Overall, the results suggest that ALF826 is a strong pharmacological anti-inflammatory agent due to CO release. In fact, ALF826 limits the expression and secretion of several pro-inflammatory agents. Thus, CO-promoted non-cell autonomous neuroprotective effect might result from limiting the inflammatory response of microglial cells.

Medium-derived from 'resting' microglia limits apoptosis in CAD neuronal cells exposed to pro-oxidant stimulus and improves neuronal morphological complexity

Other than being the CNS immune guardians, microglia have a crucial role in neuronal basal function, that range from modulation of proliferation/differentiation balance during development and trophic support, morphological and synaptic plasticity [19, 56, 57]. Moreover, to the best of our knowledge, there are no data showing CO's role in the modulation of microglia neurotrophic functions. To test the potential microglia-induced neurotrophic effect and neuroprotection, neuron-microglia conditioned media approach was used. BV2 microglial cells were treated or not with 50 μM ALF826 for 48h, then, microglial supernatant was collected for treating differentiated CAD neurons, which were simultaneously challenged with a pro-oxidant agent (*tert*-Butyl hydroperoxide, *t*-BHP) to induce neuronal cell death for 24h (Figure 5A). Conditioned medium from microglia and from CO-treated microglia, both reduced levels of neuronal death at 7.5 and 10 μM of *t*-BHP (Figure 5B). These results indicate that microglia conditioned medium, by itself, has a neuroprotective effect against oxidative stress, while CO does not further improve microglia-induced neuroprotection.

As microglia have been described to modulate neuronal network dynamics [13], it was next assessed whether CO affects neuronal morphology under basal conditions. In fact, neuronal morphology is a manner to assess neuronal function, and thus an indirectly manner to evaluate neuroprotection. CAD neurons were incubated with conditioned media from control and CO-treated microglia and stained with anti-βIII-tubulin (green) and with DAPI (nuclei staining) for morphological analysis. Microglial CO treatment modulates neuronal morphology by increasing the number of neurites *per* cell (Figure 6A), and neurite length (Figure 6B).

Overall, CO appears to stimulate microglial neurotrophic function by improving neuronal morphology under basal conditions.

CO stimulates microglial neurotrophic response

Lastly, the microglia secretome was analysed to disclose which molecular players were involved in CO-mediated microglia neuroprotection and neuronal morphological modulation. Several candidates described as key players in neurotrophism and neuronal support were assessed: BDNF (Brain-derived neurotrophic factor), GDNF (Glial cell-derived neurotrophic factor) and the anti-inflammatory cytokine IL-10. In fact, CO stimulated microglial IL-10 secretion was demonstrated by ELISA (Figure 7A). However, CO administration did not increase BDNF or GDNF secretion (data not shown). This result could point towards a neurotrophic role of CO. In fact, IL-10 overexpression is not only relevant for resolution of inflammation, but also for regulation of cell survival, neurite dynamics, development and synaptogenesis [58, 59].

Moreover, our lab has shown in the past that CO affects astrocyte-to-neuron paracrine communication, promoting neuroprotection via purinergic signalling [60]. Thus, we assessed the hypothesis that CO's regulation of microglia-neuron remote communication is partially modulated by a similar mechanism (Figure 7B). High Performance Liquid Chromatography (HPLC) showed that CO administration increased microglial adenosine levels in the supernatant (Figure 7C). Also, the protein levels of surface enzyme CD73, which converts purine mononucleotides into nucleosides, were also increased in CO-treated microglia (Figure 7D). Hence, CO may reinforce neuron-microglia communication *via* purinergic mechanisms.

Chemical inhibition of microglia-to-neuron purinergic communication reverts CO's neuroprotective properties

To validate whether the CO neuroprotective and morphogenic effect are caused by an increase in levels of adenosine in the microglial supernatant, neurons were treated with A_{2A}R antagonist SCH-58261 (1 or 5 μM) or with A_1R antagonist 8-Cyclopentyl-1,3-dipropylxanthine (DPCPX) (25 or 50 μM) and simultaneously incubated with microglia conditioned media (Figure 5A). Then, neuronal morphometric parameters and neuronal survival were analysed. Inhibition of adenosine receptors did not have any effect on neuronal survival (data not shown). Nevertheless, the increase in neurite length observed whenever CAD cells were treated with conditioned media from CO-treated microglia was reverted whenever an adenosine receptor antagonist was used (Figure 8B), indicating that the CO effect is mediated via purinergic communication. Interestingly, this effect was not A_1 or A_{2A}R specific, as both compounds reverted the CO-derived effect. Also, treating microglia with the inactivated scaffold form of ALF-826 did not have an effect on either number of neurites per cell or neurite length (Figure 8).

Discussion

In this study, we have shown that carbon monoxide (CO) modulates microglia function and impacts on microglia-to-neuron remote communication. Using a conditioned media protocol, it was demonstrated that carbon monoxide ultimately promotes indirect neuroprotection: (i) by limiting microglial pro-inflammatory reactivity and (ii) by enhancing basal microglial neurotrophism. The non-cell autonomous

effect of CO acting on microglia and promoting neuroprotection has never been described before. Furthermore, a novel Molybdenum-based CO-releasing molecule: ALF826 was used herein. This molecule presents low cytotoxicity in microglia and macrophage cell lines (Proterris (Portugal) Lda.) and delivers a large CO load.

The anti-inflammatory feature of CO has been extensively studied in macrophages [40, 61]. Likewise, microglia treated with carbon monoxide releasing molecule-3 (CORM-3) also secreted lower levels of tumour necrosis factor α (TNF-α), interleukin-1β (IL-1β) and nitrites after being triggered with different stimuli (lipopolysaccharide, thrombin and interferon γ) [38, 39]. Although there are data demonstrating the anti-neuroinflammatory role of CO in microglia, not much is known regarding direct CO modulation of neuron-microglia communication in an inflammatory setting, and how it affects neuronal survival and function.

Herein, we demonstrated that conditioned media derived from microglia treated with a pro-inflammatory stimulus (LPS) promoted neuronal cell death. Neurons challenged with inflammatory microglial supernatant partially lost morphological complexity. Moreover, microglial pre-treatment with ALF826 rescued changes in neuronal morphology and partially reverted neuronal death. Neuronal structural degradation is a marker of cell senescence and cell death in general and can be a consequence of exacerbated inflammation [62]. Alterations in neuronal network complexity are a common phenotype of neurodegenerative disorders and play a role in defective synaptic connectivity [63–66]. It has been shown that exposure of primary embryonic neurons to high levels of exogenous TNF and IL-1β alters cell morphology, affecting total arborization, number and length of dendrites, growth cone dynamics, as well as dendritic spine density and maturity [67]. Thus, loss of neuronal morphological complexity can also be partially a consequence of pro-inflammatory pathways disruption cytoskeleton signalling mechanisms, which CO could alleviate by inhibiting microglial inflammatory output. These results indicate that LPS-treated microglia drive a noxious response that causes severe neuronal damage, which can be prevented by ALF826 microglial pre-treatment.

We assessed microglial production of soluble inflammatory factors in the presence and absence of ALF826 administration. LPS increased secretion of soluble inflammatory factors TNF-α and nitrites, which were attenuated by CO administration in microglia. In contrast, LPS did not promote IL-1β release in BV2 microglia cell line (data not shown).

Despite microglia modulation of inflammation and CNS immunity, these myeloid cells also regulate brain development, synaptogenesis, neuronal turnover and provide strong neurotrophic support to neuronal cells [12, 19, 69, 20–24, 56, 57, 68]. Interestingly, CO modulation of microglial neurotrophic response has never been explored. Herein, we showed that conditioned media derived from non-activated microglia protected neurons from oxidative damage by partially preventing neuronal cell death. Microglia neuroprotection can result from secretion of neurotrophins (BDNF, Neurotrophin-3, Nerve growth factor) [20, 70], inflammatory cytokines [24] or survival growth factors (IGF-1) [12], which impact cell fate. In the present work, CO did not increase microglial production and secretion of BDNF or GDNF, while IL-10

release was stimulated by CO. Microglial IL-10 is a key anti-inflammatory regulator, anti-apoptotic and an important synaptogenic mediator *in vivo* [71–73]. Accordingly, using *in vivo* acute inflammation model and *in vitro* LPS-stimulated macrophages, CO promoted IL-10 production [40]. Under physiological conditions without inflammatory stimulation, this is the first work showing CO-induced production of IL-10 in microglia. Furthermore, IL-10 promotes neurite outgrowth and synapse formation in OGD (Oxygen-glucose deprivation)-challenged primary cortical neurons[59]. Herein, conditioned medium from CO-treated microglia increased number of neurites per cell and neurite length. Because IL-10 has a neuromorphogenic role [59], one may speculate that IL-10 is involved in neuronal morphology improvement by reinforcing neurotrophism.

Moreover, we unveiled that CO acts as a stimulator of microglia purinergic signalling, which affects neuronal function and survival. Purinergic signalling is important for cellular cross-talk and both microglial environmental sensing and reactivity [74], as well as neuronal survival and function [75]. Activation of adenosine receptor A_{2A} has been reported to promote axonal elongation and dendritic branching in cortical neurons [76]. A recent breakthrough paper has shown that microglia can sense neuronal ATP, convert it into adenosine, which acts as an important suppressant of neuronal activity and overall animal behaviour [17]. We have previously shown similar results concerning astrocyte to neuron communication. Namely, CO-treated astrocytes provided neuroprotection and increased neuronal viability in a co-culture model by enhancing release and conversion of ATP into adenosine [60].

Interestingly, previous reports have also shown upregulation of ectonucleotidases following brain ischemia, providing cerebral protection [77]. In microglia, CD39 and CD73 is crucial for microglial ramification, phagocytosis, and motility [78] and *in vitro* silencing of CD73 in BV2 microglia results in a clear pro-inflammatory profile [79]. Furthermore, CD73 expression is relevant for microglial polarization and inflammatory attenuation in a spinal cord injury model [79]. This data could indicate that there is a paracrine feedback loop in microglia in which secreted ATP is converted into adenosine and recognized by the self, thus regulating microglial inflammatory activity. Herein, chemical inhibition of neuronal adenosine indicates that microglial adenosine has a direct effect on neuronal function, but we cannot exclude that CO also regulates microglial CD73 expression, increasing adenosine levels in the supernatant, priming microglia to release higher levels of other neuroactive compounds. This would be in accordance with existing results, that claim that CD73 activity drives microglia towards an M2 profile by autocrine A_{2B} agonism. Further experiments are needed to assess this hypothesis.

In summary, neurotrophic factors, anti-oxidant molecules or even anti-apoptotic players can be involved in microglia-induced neuroprotection under non-inflammatory conditions.

Conclusion

Taken together, ALF826 is a promising new CO releasing molecule that limits microglial reactivity and secretion of inflammatory mediators, and that improves the release of neurotrophic factors. Both effects protect neurons against cell death and improve neuronal morphology. In fact and to the best of our

knowledge, this is the first report showing that CO affects basal microglia function, by stimulating neurotrophism. Hence, CO regulates neuron-microglia remote communication and promotes neuroprotection in a non-cell autonomous manner by both limiting inflammation and improving neurotrophism. The novel ALF826 has also proven to be a useful CORM for the reproducible and non-toxic delivery of CO enabling the study of intercellular processes and with potential for future clinical applications.

Abbreviations

BDNF : brain-derived neurotrophic factor; CO: Carbon monoxide; CORM: Carbon monoxide releasing molecules; CNS: Central Nervous System; DPCPX: Dipropylcyclopentylxanthine; H2DCFDA: 2',7'-dichlorofluorescein diacetate; ERK: extracellular-signal-regulated kinase; FBS: foetal bovine serum; GDNF: glial cell-derived neurotrophic factor; HO: haem oxygenase; IGF-1: insulin growth factor 1; IFN-γ: interferon γ induced; IL-1β: interleukin-1β; IL-10: interleukin-10; LPS: lipopolysaccharide; NLRP3: NLR Family Pyrin Domain Containing 3; NO: nitric oxide; PFA: paraformaldehyde; PDL: Poly-D-Lysine; PPAR-γ: Peroxisome proliferator-activated receptor gamma co-activator 1 α; PI3K: Phosphoinositide 3-kinase; ROS: reactive oxygen species; RT: room temperature; SDS-PAGE: sodium dodecyl sulphate–polyacrylamide gel electrophoresis; *t*-BHP: *tert*-Butyl hydroperoxide and TNF-α: Tumour necrosis factor α.

Declarations

Acknowledgments

This work was financed by FEDER - Fundo Europeu de Desenvolvimento Regional funds through the COMPETE 2020 - Operational Programme for Competitiveness and Internationalization (POCI), Portugal 2020, and by Portuguese funds through FCT - Fundação para a Ciência e a Tecnologia/Ministério da Ciência (FCT), Tecnologia e Ensino Superior in the framework of FCT-ANR/NEU-NMC/0022/2012 grant, PTDC/MEC-NEU/28750/2017 grant, Applied Molecular Biosciences Unit-UCIBIO (UID/Multi/04378/2019) grant; iNOVA4Health - Programme in Translational Medicine (UID/Multi/04462/2013) grant and LA/P/0140/2020 of the Associate Laboratory Institute for Health and Bioeconomy; and FCT provided individual financial support NLS (PD/BD/127819/2016), BFM (PD/BD/128336/2017) and HLAV (IF/00185/2012).

Ethics approval and consent to participate

All animal experiments were performed with the approval of the i3S Animal Ethics Committee and in accordance with European Union Directive on the protection of animals used for scientific purposes (2010/63/EU) and the Portuguese Law that transposes it (Decreto-Lei n.º 113/2013). All efforts were made to minimize animal suffering.

Funding

This work was financed by FEDER - Fundo Europeu de Desenvolvimento Regional funds through the COMPETE 2020 - Operational Programme for Competitiveness and Internationalization (POCI), Portugal 2020, and by Portuguese funds through FCT - Fundação para a Ciência e a Tecnologia/Ministério da Ciência (FCT), Tecnologia e Ensino Superior in the framework of FCT-ANR/NEU-NMC/0022/2012 grant, PTDC/MEC-NEU/28750/2017 grant, Applied Molecular Biosciences Unit-UCIBIO (UID/Multi/04378/2019) grant; iNOVA4Health - Programme in Translational Medicine (UID/Multi/04462/2013) grant and LA/P/0140/2020 of the Associate Laboratory Institute for Health and Bioeconomy; and FCT provided individual financial support NLS (PD/BD/127819/2016), BFM (PD/BD/128336/2017) and HLAV (IF/00185/2012).

Consent for publication

All authors agreed to the publication of this manuscript.

Availability of data and materials

The datasets generated during and/or analysed during the current study are available from the corresponding author on a reasonable request.

Authors' contributions

NLS designed the study, conducted the experiments, helped with data analysis and evaluation, wrote the manuscript, and approved the final version of this manuscript. IP conducted the experiments, helped with data analysis and approved the final version of this manuscript. JB helped with primary cultures and approved the final version of this manuscript. CSFQ designed part of the study, conducted some of the experiments and approved the final version of this manuscript. BFM and SVC helped with HPLC experiments and data analysis and approved the final version of this manuscript. CCR provided the CORM ALF-826 (which is not available commercially), helped with data analysis and approved the final version of this manuscript. TS designed part of the study, helped with data analysis and approved the final version of this manuscript. HLAV designed the study, helped with data analysis and evaluation, wrote the manuscript and approved the final version of this manuscript.

Competing interests

The co-author Carlos C. Romão is a scientific consultant of Proterris (Portugal) Lda, and has an equity position in the company.

References

1. Kettenmann H, Hanisch U-K, Noda M, Verkhratsky A (2011) Physiology of microglia. Physiol Rev 91:461–553 . doi: 10.1152/physrev.00011.2010

2. Ginhoux F, Greter M, Leboeuf M, et al (2010) Fate Mapping Analysis Reveals That Adult Microglia Derive from Primitive Macrophages. Science (80-) 330:841–845 . doi: 10.1126/science.1194637

3. Salter MW, Stevens B (2017) Microglia emerge as central players in brain disease. Nat Med 23:1018–1027 . doi: 10.1038/nm.4397

4. Colton CA, Gilbert DL (1987) Production of superoxide anions by a CNS macrophage, the microglia. FEBS Lett 223:284–288

5. Infanger DW, Sharma R V., Davisson RL (2006) NADPH Oxidases of the Brain: Distribution, Regulation, and Function. Antioxid Redox Signal 8:1583–1596 . doi: 10.1089/ars.2006.8.1583

6. Neniskyte U, Vilalta A, Brown GC (2014) Tumour necrosis factor alpha-induced neuronal loss is mediated by microglial phagocytosis. FEBS Lett 588:2952–2956 . doi: 10.1016/j.febslet.2014.05.046

7. Sedel F, Béchade C, Vyas S, Triller A (2004) Macrophage-Derived Tumor Necrosis Factor α, an Early Developmental Signal for Motoneuron Death. J Neurosci. doi: 10.1523/JNEUROSCI.4464-03.2004

8. Paolicelli RC, Bergamini G, Rajendran L (2019) Cell-to-cell Communication by Extracellular Vesicles: Focus on Microglia. Neuroscience 405

9. Neumann H, Kotter MR, Franklin RJM (2009) Debris clearance by microglia: An essential link between degeneration and regeneration. Brain 132:288–295

10. Neher JJ, Emmrich J V., Fricker M, et al (2013) Phagocytosis executes delayed neuronal death after focal brain ischemia. Proc Natl Acad Sci 110:E4098–E4107 . doi: 10.1073/pnas.1308679110

11. Ellwardt E, Walsh JT, Kipnis J, Zipp F (2016) Understanding the Role of T Cells in CNS Homeostasis. Trends Immunol.

12. Arnoux I, Hoshiko M, Sanz Diez A, Audinat E (2014) Paradoxical effects of minocycline in the developing mouse somatosensory cortex. Glia. doi: 10.1002/glia.22612

13. Mosser CA, Baptista S, Arnoux I, Audinat E (2017) Microglia in CNS development: Shaping the brain for the future. Prog Neurobiol 149–150:1–20 . doi: 10.1016/j.pneurobio.2017.01.002

14. Paolicelli RC, Bolasco G, Pagani F, et al (2011) Synaptic pruning by microglia is necessary for normal brain development. Science (80-). doi: 10.1126/science.1202529

15. Schafer DP, Lehrman EK, Kautzman AG, et al (2012) Microglia Sculpt Postnatal Neural Circuits in an Activity and Complement-Dependent Manner. Neuron. doi: 10.1016/j.neuron.2012.03.026

16. Tremblay MĚ, Lowery RL, Majewska AK (2010) Microglial interactions with synapses are modulated by visual experience. PLoS Biol. doi: 10.1371/journal.pbio.1000527

17. Badimon A, Strasburger HJ, Ayata P, et al (2020) Negative feedback control of neuronal activity by microglia. Nature 586: . doi: 10.1038/s41586-020-2777-8

18. Miyamoto A, Wake H, Ishikawa AW, et al (2016) Microglia contact induces synapse formation in developing somatosensory cortex. Nat Commun. doi: 10.1038/ncomms12540

19. Tremblay MÈ, Stevens B, Sierra A, et al (2011) The role of microglia in the healthy brain. J Neurosci. doi: 10.1523/JNEUROSCI.4158-11.2011

20. Morgan SC, Taylor DL, Pocock JM (2004) Microglia release activators of neuronal proliferation mediated by activation of mitogen-activated protein kinase, phosphatidylinositol-3-kinase/ Akt and delta-Notch signalling cascades. J Neurochem 90:89–101

21. Nagata K, Takei N, Nakajima K, et al (1993) Microglial conditioned medium promotes survival and development of cultured mesencephalic neurons from embryonic rat brain. J Neurosci Res. doi: 10.1002/jnr.490340313

22. Chamak B, Dobbertin A, Mallat M (1995) Immunohistochemical detection of thrombospondin in microglia in the developing rat brain. Neuroscience. doi: 10.1016/0306-4522(95)00236-C

23. Arnoux I, Hoshiko M, Mandavy L, et al (2013) Adaptive phenotype of microglial cells during the normal postnatal development of the somatosensory “Barrel” cortex. Glia. doi: 10.1002/glia.22503

24. Shigemoto-Mogami Y, Hoshikawa K, Goldman JE, et al (2014) Microglia enhance neurogenesis and oligodendrogenesis in the early postnatal subventricular zone. J Neurosci. doi: 10.1523/JNEUROSCI.1619-13.2014

25. Parkhurst CN, Yang G, Ninan I, et al (2013) Microglia promote learning-dependent synapse formation through brain-derived neurotrophic factor. Cell. doi: 10.1016/j.cell.2013.11.030

26. Lim SH, Park E, You B, et al (2013) Neuronal synapse formation induced by microglia and interleukin 10. PLoS One. doi: 10.1371/journal.pone.0081218

27. Pascual O, Achour S Ben, Rostaing P, et al (2012) Microglia activation triggers astrocyte-mediated modulation of excitatory neurotransmission. Proc Natl Acad Sci U S A. doi: 10.1073/pnas.1111098109

28. Poon VY, Choi S, Park M (2013) Growth factors in synaptic function. Front. Synaptic Neurosci.

29. Heneka MTM, Carson MJ, Khoury JEJ El, et al (2015) Neuroinflammation in Alzheimer’s disease. Lancet Neurol. doi: 10.1016/S1474-4422(15)70016-5

30. Hu X, Li P, Guo Y, et al (2012) Microglia/macrophage polarization dynamics reveal novel mechanism of injury expansion after focal cerebral ischemia. Stroke 43:3063–3070 . doi: 10.1161/STROKEAHA.112.659656

31. Tenhunen R, Marver HS, Schmid R (1968) The enzymatic conversion of heme to bilirubin by microsomal heme oxygenase. Proc Natl Acad Sci 61:748–755 . doi: 10.1073/pnas.61.2.748

32. Ryter SW, Alam J, Choi AMK (2006) Heme Oxygenase-1/Carbon Monoxide: From Basic Science to Therapeutic Applications. Physiol Rev 86:583–650 . doi: 10.1152/physrev.00011.2005

33. Ryter SW, Choi AMK (2016) Targeting heme oxygenase-1 and carbon monoxide for therapeutic modulation of inflammation. Transl. Res. 167:7–34

34. Figueiredo-Pereira C, Dias-Pedroso D, Soares NL, Vieira HLA (2020) CO-mediated cytoprotection is dependent on cell metabolism modulation. Redox Biol. 32

35. Queiroga CSF, Vercelli A, Vieira HLA (2015) Carbon monoxide and the CNS: challenges and achievements. Br J Pharmacol 172:1533–1545 . doi: 10.1111/bph.12729

36. Bilban M, Bach FH, Otterbein SL, et al (2006) Carbon Monoxide Orchestrates a Protective Response through PPARγ. Immunity 24:601–610 . doi: 10.1016/j.immuni.2006.03.012

37. Hoetzel A, Dolinay T, Vallbracht S, et al (2008) Carbon monoxide protects against ventilator-induced lung injury via PPAR-γ and inhibition of Egr-1. Am J Respir Crit Care Med 177:1223–1232 . doi: 10.1164/rccm.200708-1265OC

38. Bani-Hani MG, Greenstein D, Mann BE, et al (2006) Modulation of thrombin-induced neuroinflammation in BV-2 microglia by carbon monoxide-releasing molecule 3. J Pharmacol Exp Ther 318:1315–1322 . doi: 10.1124/jpet.106.104729

39. Peyton KJ, Reyna S V, Chapman GB, et al (2002) Heme oxygenase-1 – derived carbon monoxide is an autocrine inhibitor of vascular smooth muscle cell growth. Blood 99:4443–4448

40. Otterbein LE, Bach FH, Alam J, et al (2000) Carbon monoxide has anti-inflammatory effects involving the mitogen-activated protein kinase pathway. Nat Med 6:422–8 . doi: 10.1038/74680

41. Vieira HLAAHLA, Queiroga CSFCSFCSFF, Alves PMPM (2008) Pre-conditioning induced by carbon monoxide provides neuronal protection against apoptosis. J Neurochem 107:375–384 . doi: 10.1111/j.1471-4159.2008.05610.x

42. Schallner N, Romão CC, Biermann J, et al (2013) Carbon Monoxide Abrogates Ischemic Insult to Neuronal Cells via the Soluble Guanylate Cyclase-cGMP Pathway. PLoS One 8: . doi: 10.1371/journal.pone.0060672

43. Wang B, Cao W, Biswal S, Doré S (2011) Carbon monoxide-activated Nrf2 pathway leads to protection against permanent focal cerebral ischemia. Stroke 42:2605–2610 . doi: 10.1161/STROKEAHA.110.607101

44. Queiroga CSF, Tomasi S, Widerøe M, et al (2012) Preconditioning Triggered by Carbon Monoxide (CO) Provides Neuronal Protection Following Perinatal Hypoxia-Ischemia. PLoS One 7: . doi: 10.1371/journal.pone.0042632

45. Queiroga CSF, Almeida AS, Martel C, et al (2010) Glutathionylation of Adenine Nucleotide Translocase Induced by Carbon Monoxide Prevents Mitochondrial Membrane Permeabilization and Apoptosis. J Biol Chem 285:17077–17088 . doi: 10.1074/jbc.M109.065052

46. Almeida AS, Queiroga CSF, Sousa MFQ, et al (2012) Carbon monoxide modulates apoptosis by reinforcing oxidative metabolism in astrocytes: Role of Bcl-2. J Biol Chem 287:10761–10770 . doi: 10.1074/jbc.M111.306738

47. Oliveira SR, Figueiredo-Pereira C, Duarte CB, Vieira HLA (2019) P2X7 Receptors Mediate CO-Induced Alterations in Gene Expression in Cultured Cortical Astrocytes—Transcriptomic Study. Mol Neurobiol 56:3159–3174 . doi: 10.1007/s12035-018-1302-7

48. Parfenova H, Tcheranova D, Basuroy S, et al (2012) Functional role of astrocyte glutamate receptors and carbon monoxide in cerebral vasodilation response to glutamate. AJP Hear Circ Physiol 302:H2257–H2266 . doi: 10.1152/ajpheart.01011.2011

49. Bani-Hani MG, Greenstein D, Mann BE, et al (2006) A carbon monoxide-releasing molecule (CORM-3) attenuates lipopolvsaccharide- And interferon-γ-induced inflammation in microglia. Pharmacol. Reports 58:132–144

50. Wilson JLJL, Bouillaud F, Almeida ASAS, et al (2017) Carbon monoxide reverses the metabolic adaptation of microglia cells to an inflammatory stimulus. Free Radic Biol Med 104:311–323 . doi: 10.1016/j.freeradbiomed.2017.01.022

51. Chora AA, Fontoura P, Cunha A, et al (2007) Heme oxygenase-1 and carbon monoxide suppress autoimmune neuroinflammation. J Clin Invest 117:438–447 . doi: 10.1172/JCI28844

52. Yabluchanskiy A, Sawle P, Homer-Vanniasinkam S, et al (2012) CORM-3, a carbon monoxide-releasing molecule, alters the inflammatory response and reduces brain damage in a rat model of hemorrhagic stroke. Crit Care Med 40:544–552 . doi: 10.1097/CCM.0b013e31822f0d64

53. Motterlini R, Clark JE, Foresti R, et al (2002) Carbon monoxide-releasing molecules: characterization of biochemical and vascular activities. Circ Res 90:e17–e24 . doi: 10.1161/hh0202.104530

54. Johnson TR, Mann BE, Clark JE, et al (2003) Metal carbonyls: A new class of pharmaceuticals? Angew. Chemie - Int. Ed.

55. Motterlini R, Sawle P, Hammad J, et al (2005) CORM-A1: a new pharmacologically active carbon monoxide-releasing molecule. Faseb J 19:284–286 . doi: 10.1096/fj.04-2169fje

56. Kettenmann H, Kirchhoff F, Verkhratsky A (2013) Microglia: New Roles for the Synaptic Stripper. Neuron

57. Frost JL, Schafer DP (2016) Microglia: Architects of the Developing Nervous System. Trends Cell Biol.

58. Pérez-De Puig I, Miró F, Salas-Perdomo A, et al (2013) IL-10 deficiency exacerbates the brain inflammatory response to permanent ischemia without preventing resolution of the lesion. J Cereb Blood Flow Metab 33: . doi: 10.1038/jcbfm.2013.155

59. Chen H, Lin W, Zhang Y, et al (2016) IL-10 Promotes Neurite Outgrowth and Synapse Formation in Cultured Cortical Neurons after the Oxygen-Glucose Deprivation via JAK1/STAT3 Pathway. Sci Rep 6: . doi: 10.1038/srep30459

60. Queiroga CSFCSFCSF, Alves RMARMARMA, Conde SVSVS V., et al (2016) Paracrine effect of carbon monoxide: astrocytes promote neuroprotection via purinergic signaling. J Cell Sci 129:3178–88 . doi: 10.1242/jcs.187260

61. Sawle P, Foresti R, Mann BE, et al (2005) Carbon monoxide-releasing molecules (CO-RMs) attenuate the inflammatory response elicited by lipopolysaccharide in RAW264.7 murine macrophages. Br J Pharmacol 145:800–810 . doi: 10.1038/sj.bjp.0706241

62. Galluzzi L, Vitale I, Aaronson SA, et al (2018) Molecular mechanisms of cell death: Recommendations of the Nomenclature Committee on Cell Death 2018. Cell Death Differ. 25

63. Yuan TF, Peng B, Machado S, Arias-Carrion O (2015) Morphological Bases of Neuronal Hyperexcitability in Neurodegeneration. CNS Neurosci. Ther. 21

64. Ferrer I (1999) Neurons and their dendrites in frontotemporal dementia. Dement Geriatr Cogn Disord 10: . doi: 10.1159/000051214

65. Spires TL, Hyman BT (2004) Neuronal structure is altered by amyloid plaques. Rev. Neurosci. 15

66. Šišková Z, Justus D, Kaneko H, et al (2014) Dendritic structural degeneration is functionally linked to cellular hyperexcitability in a mouse model of alzheimer's disease. Neuron 84: . doi: 10.1016/j.neuron.2014.10.024

67. Frias, Cátia; Brites, Dora; Fernandes A (2011) Cátia Sofia Pereira Frias Dissecting neuronal development deficits by inflammation : from morphology to cytoskeleton dynamics. Faculdade de Farmácia da Universidade de Lisboa

68. Cunningham CL, Martínez-Cerdeño V, Noctor SC (2013) Microglia regulate the number of neural precursor cells in the developing cerebral cortex. J Neurosci. doi: 10.1523/JNEUROSCI.3441-12.2013

69. Antony JM, Paquin A, Nutt SL, et al (2011) Endogenous microglia regulate development of embryonic cortical precursor cells. J Neurosci Res. doi: 10.1002/jnr.22533

70. Frade JM, Barde YA (1998) Microglia-derived nerve growth factor causes cell death in the developing retina. Neuron 20: . doi: 10.1016/S0896-6273(00)80432-8

71. Bachis A, Colangelo AM, Vicini S, et al (2001) Interleukin-10 prevents glutamate-mediated cerebellar granule cell death by blocking caspase-3-like activity. J Neurosci 21: . doi: 10.1523/jneurosci.21-09-03104.2001

72. Sawada M, Suzumura A, Hosoya H, et al (1999) Interleukin-10 inhibits both production of cytokines and expression of cytokine receptors in microglia. J Neurochem 72: . doi: 10.1046/j.1471-4159.1999.721466.x

73. Lodge PA, Sriram S (1996) Regulation of microglial activation by TGF-β, IL-10, and CSF-1. J Leukoc Biol 60: . doi: 10.1002/jlb.60.4.502

74. Illes P, Rubini P, Ulrich H, et al (2020) Regulation of Microglial Functions by Purinergic Mechanisms in the Healthy and Diseased CNS. Cells 9

75. Fields RD, Burnstock G (2006) Purinergic signalling in neuron-glia interactions. Nat Rev Neurosci 7:423–436

76. Assaife-Lopes N, Sousa VC, Pereira DB, et al (2010) Activation of adenosine A2A receptors induces TrkB translocation and increases BDNF-mediated phospho-TrkB localization in lipid rafts: Implications for neuromodulation. J Neurosci 30: . doi: 10.1523/JNEUROSCI.5695-09.2010

77. Shinozaki Y, Koizumi S, Ishida S, et al (2005) Cytoprotection against oxidative stress-induced damage of astrocytes by extracellular ATP via P2Y1 receptors. Glia 49:288–300

78. Matyash M, Zabiegalov O, Wendt S, et al (2017) The adenosine generating enzymes CD39/CD73 control microglial processes ramification in the mouse brain. PLoS One 12: . doi: 10.1371/journal.pone.0175012

79. Xu S, Zhu W, Shao M, et al (2018) Ecto-5'-nucleotidase (CD73) attenuates inflammation after spinal cord injury by promoting macrophages/microglia M2 polarization in mice. J Neuroinflammation 15: . doi: 10.1186/s12974-018-1183-8

Figures

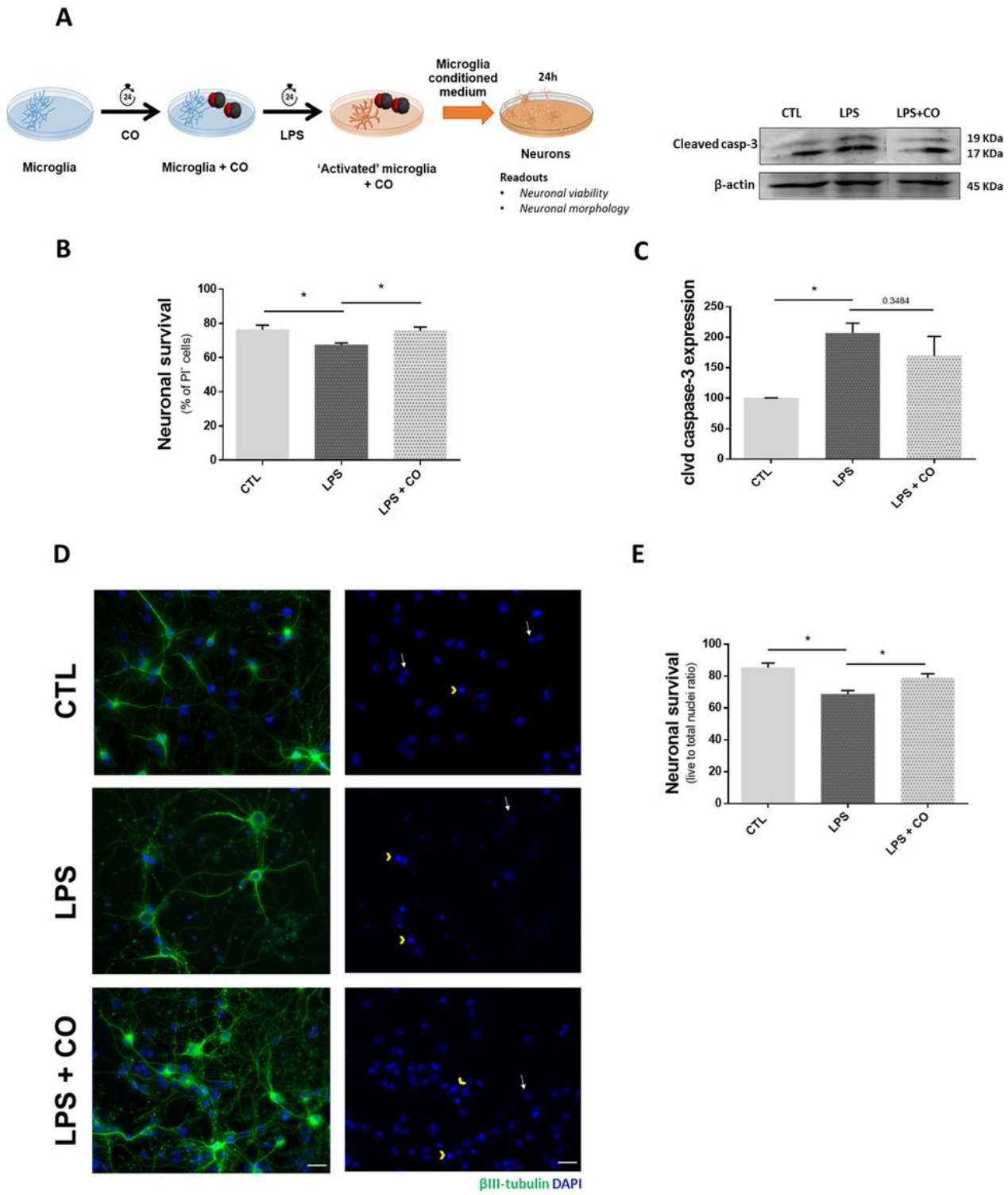

Figure 1

Carbon monoxide (CO) treatment in microglia attenuates neuronal cell death induced by conditioned medium from LPS-activated microglia. BV2 microglia were treated with ALF826 (50 μM) for 24 hours and with LPS (500 ng/mL) for another 24 hours. “Activated” microglia are cells treated with LPS. CAD neuronal culture was subsequently incubated with microglia conditioned medium (A). Cell viability was assessed by (B) propidium iodide staining quantification in flow cytometry or by (C) cleaved caspase 3

protein expression by Western Blotting. The densitometry of cleaved caspase-3 expression was normalized for β-actin and is presented as percentage relative to the control. Representative membranes for the experiments are displayed (C). n=4, error bars represent mean ± SEM, *p<0.05 by one-way ANOVA test. CO provides neuroprotection in primary hippocampal neurons via modulation of primary microglia. Rat hippocampal neurons were challenged with conditioned medium from primary microglia cells for 24 hours and immunostained with βIII-tubulin primary antibody (green) and DAPI (nuclei in blue) (D, scale bar = 25 μm). Cell viability was assessed by counting total and apoptotic neurons. White arrows highlight the nucleus of live neurons and yellow arrowheads highlight the nucleus of dead neurons. The live/total nuclei ratio was registered and is presented in (E). n=3, error bars represent mean ± SEM, *p<0.05 by one-way ANOVA test.

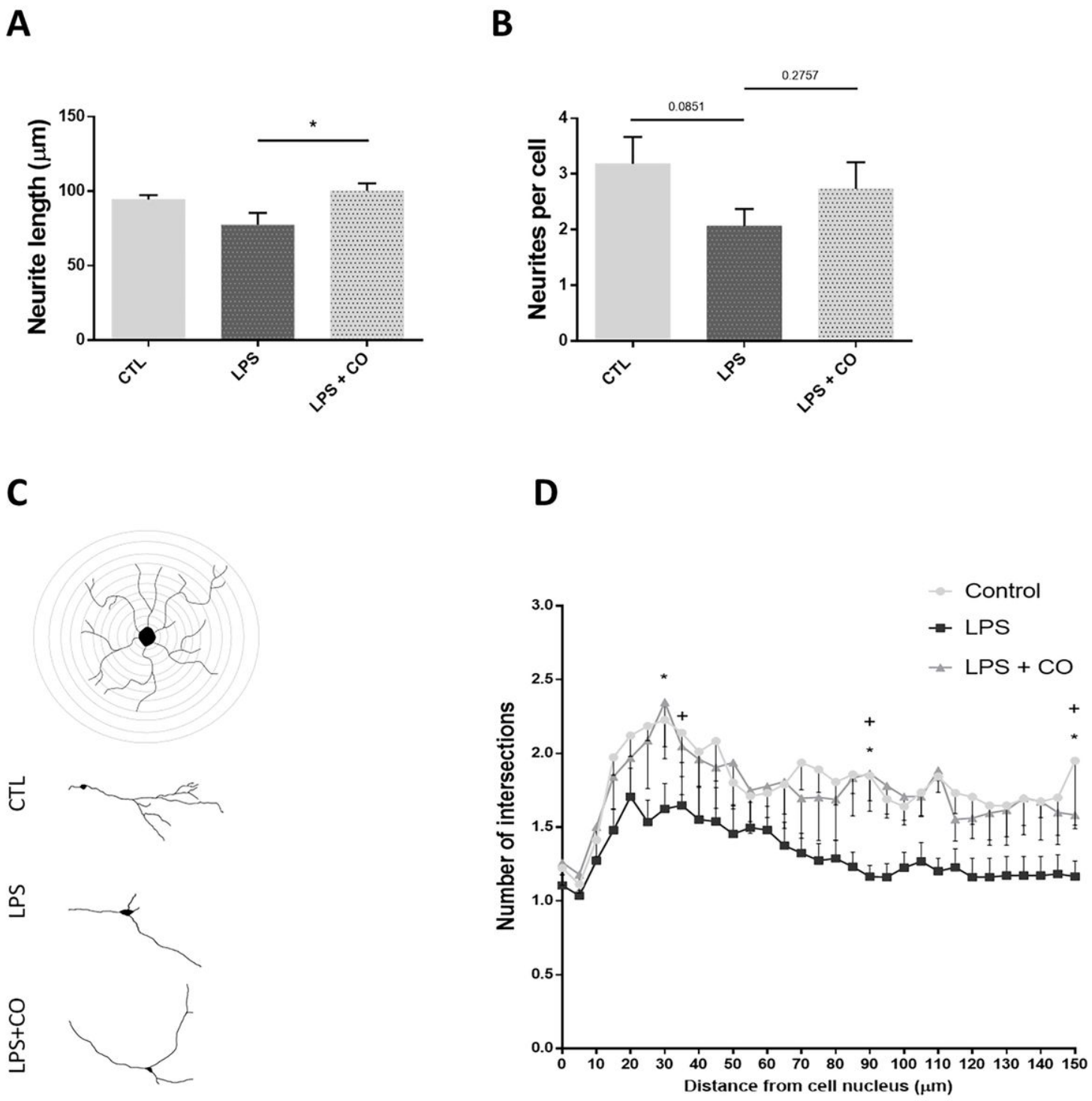

Figure 2

Administration of CO in microglia limits loss of morphological complexity in neurons exposed to LPS-activated microglia conditioned medium. CAD neurons treated with BV2 microglia conditioned media for 24h were immunostained with a βIII-tubulin antibody. Nuclei were stained with DAPI. Following image acquisition, morphological features, such as (A) neurite length, (B) number of neurites per cell and (D) Sholl analysis were assessed from six independent experiments (10-15 cells per condition).

Representative tracings of 2D acquired images were also performed (C). n=5-6, error bars represent mean ± SEM, * (CTL vs LPS) and + (LPSCO vs LPS) p<0.05 by one-way ANOVA test.

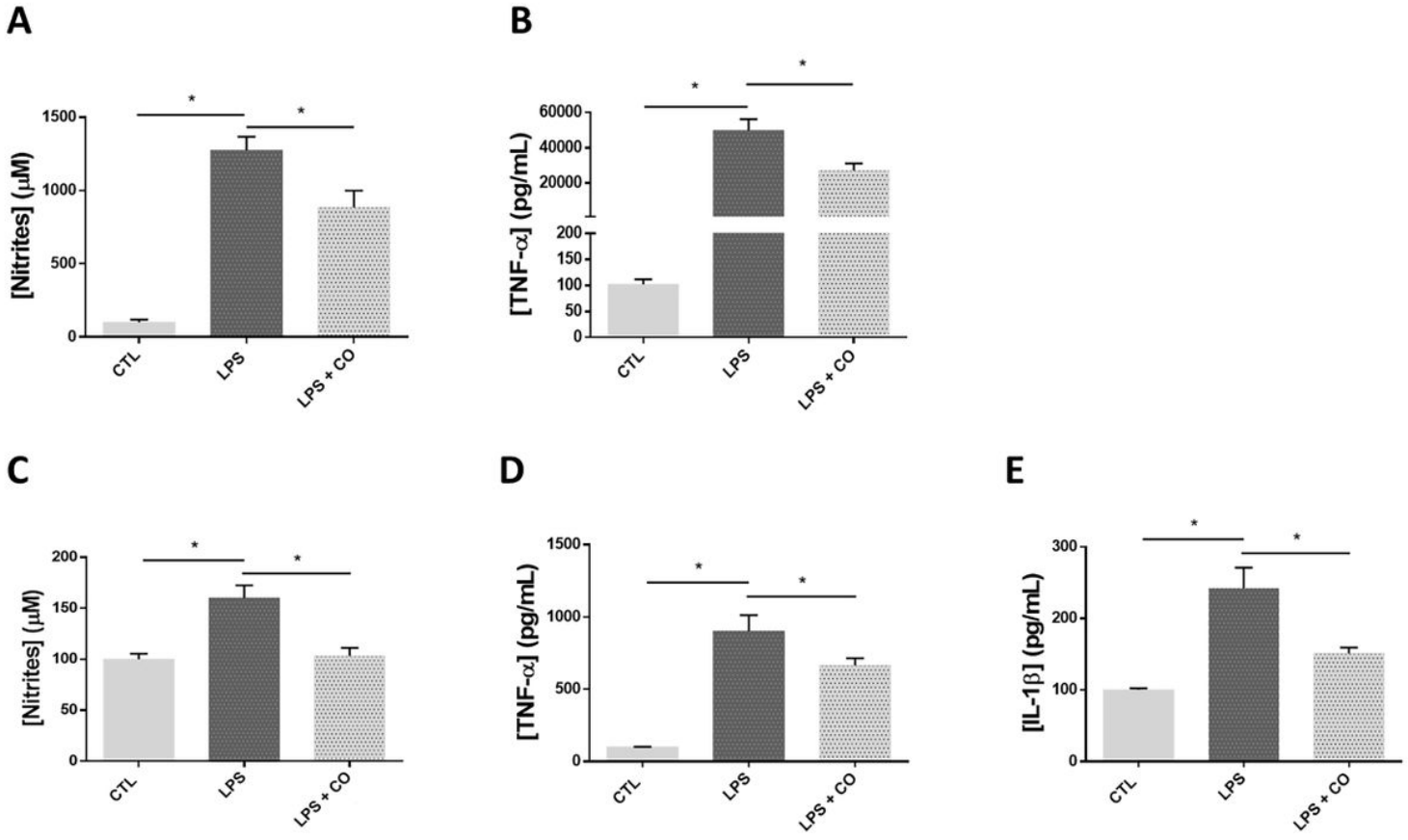

Figure 3

CO attenuates the inflammatory profile of microglia's secretome. BV2 microglia supernatant was quantified for nitrite levels (A) by Griess colorimetric assay. TNF-α (B) was assessed via ELISA. All results are presented as percentage relative to the negative control. n=5-6, error bars represent mean ± SEM, *p<0.05 by one-way ANOVA. CO treatment inhibits the inflammatory secretome of primary microglial cells. Supernatant from rat primary microglia was collected and secretome was analysed. (C) Nitrite quantification was performed via Griess colorimetric assay and ELISA assays were utilized for the quantification of TNF-α (D) and IL-1ß (E) levels. All data is presented as percentage relative to the negative control. n=3, error bars represent mean ± SEM, *p<0.05 by one-way ANOVA.

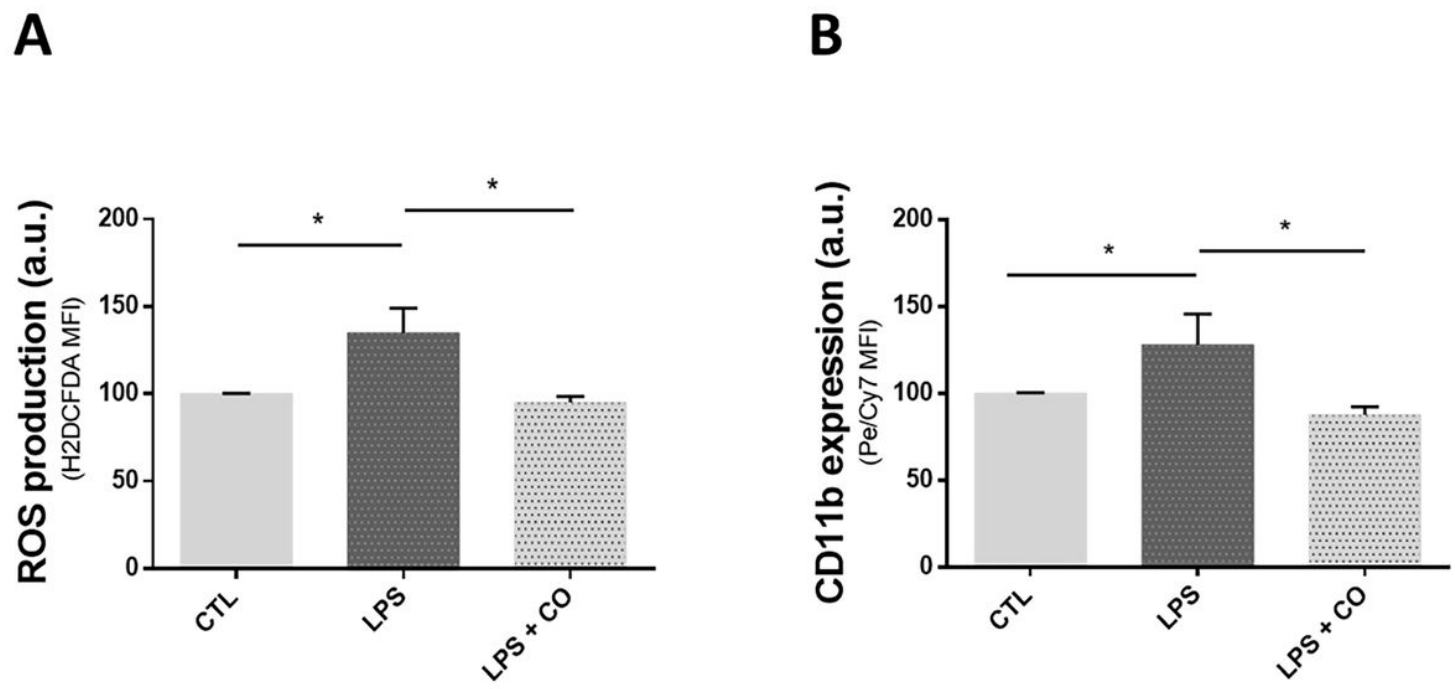

Figure 4

CO decreases microglial expression of inflammatory reactivity markers. BV2 microglia cells were collected, and expression of inflammatory markers was assessed. (A) Intracellular H2O2 levels were measured by fluorescence using H(2)DCF-DA and normalized to total protein levels. (B) CD11b surface expression was quantified by Pe/Cy7 immunofluorescence median fluorescence intensity via flow cytometry. Results in (A) and (B) are presented as percentage relative to the negative control. n=3-5, error bars represent mean ± SEM, *p<0.05 by one-way ANOVA test.

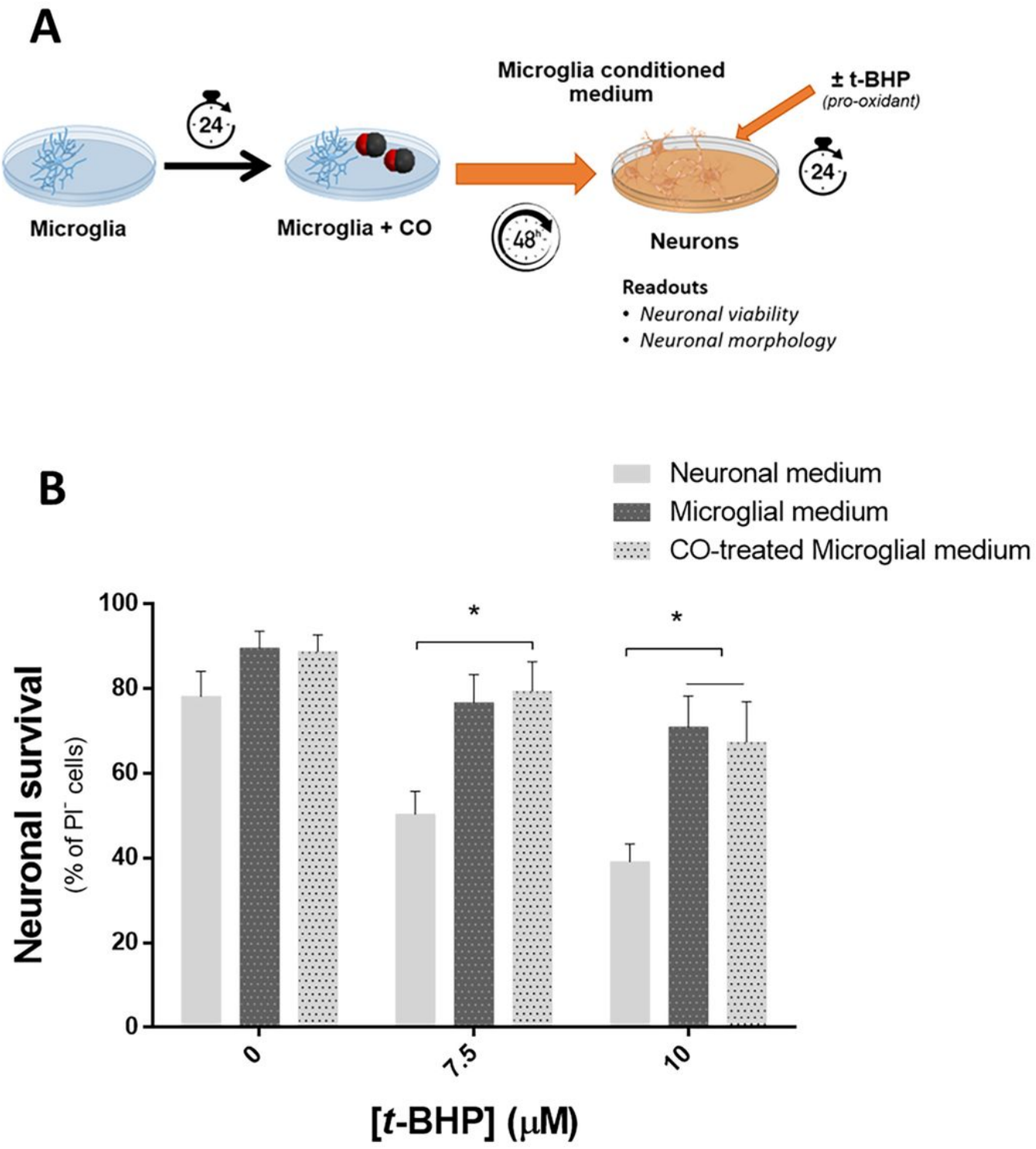

Figure 5

Microglia conditioned media provides a protective effect in neurons exposed to oxidative stress. BV2 microglia were treated with ALF826 (50 μM) for 48 hours. CAD neuronal culture was simultaneously incubated with microglia conditioned medium and with pro-oxidant agent t-BHP (A). Cell viability was assessed by (B) propidium iodide staining quantification in flow cytometry. n=6, error bars represent mean ± SEM, *p<0.05 by one-way ANOVA test.

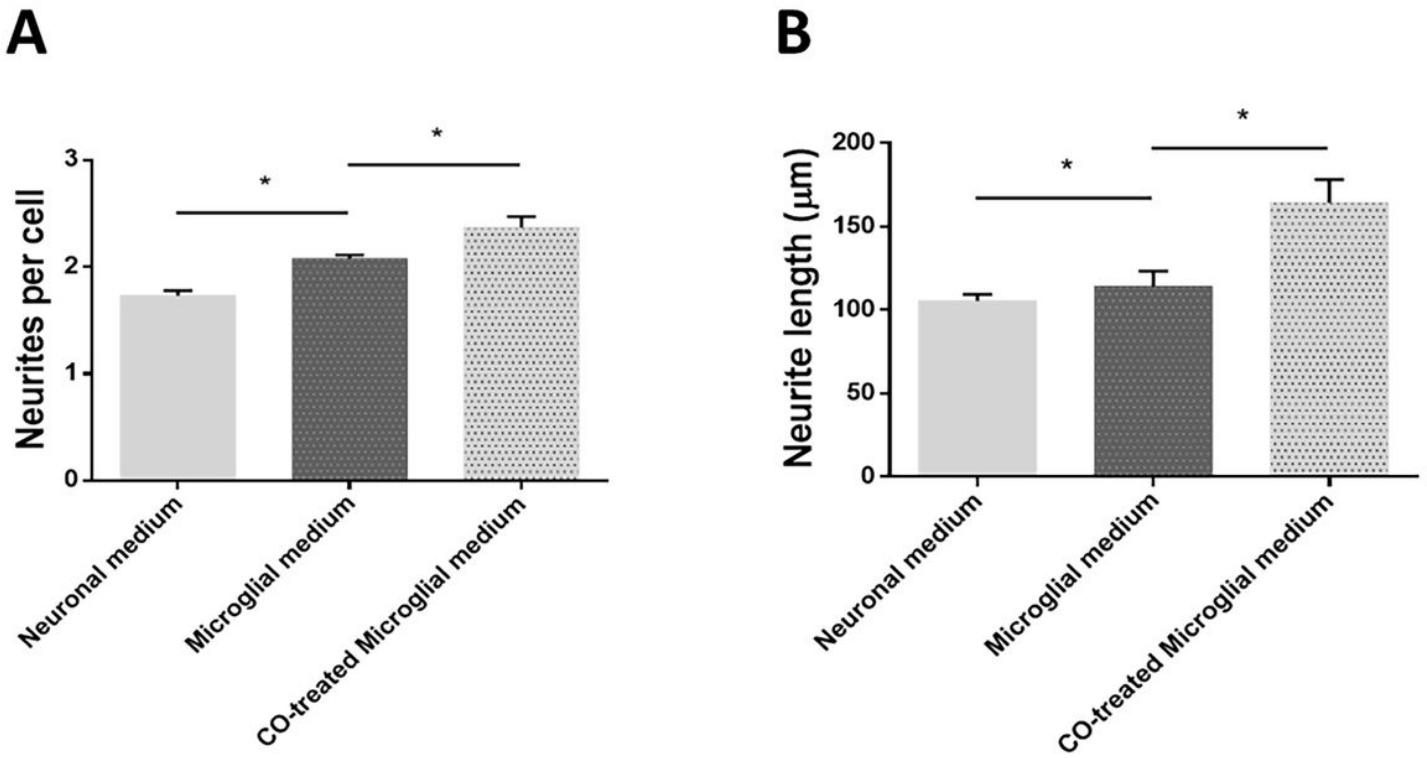

Figure 6

Administration of CO in ‘resting’ microglia increases neuronal morphological complexity after exposure to conditioned medium. CAD neurons treated with BV2 microglia conditioned media for 24h were labelled with a βIII-tubulin antibody and DAPI, and fluorescence microscopy was performed. Micrographs were analysed and morphological features (A) number of neurites per cell and (B) neurite length were assessed from five independent experiments (10-15 cells per condition). n=5, error bars represent mean ± SEM, *p<0.05 by one-way ANOVA test.

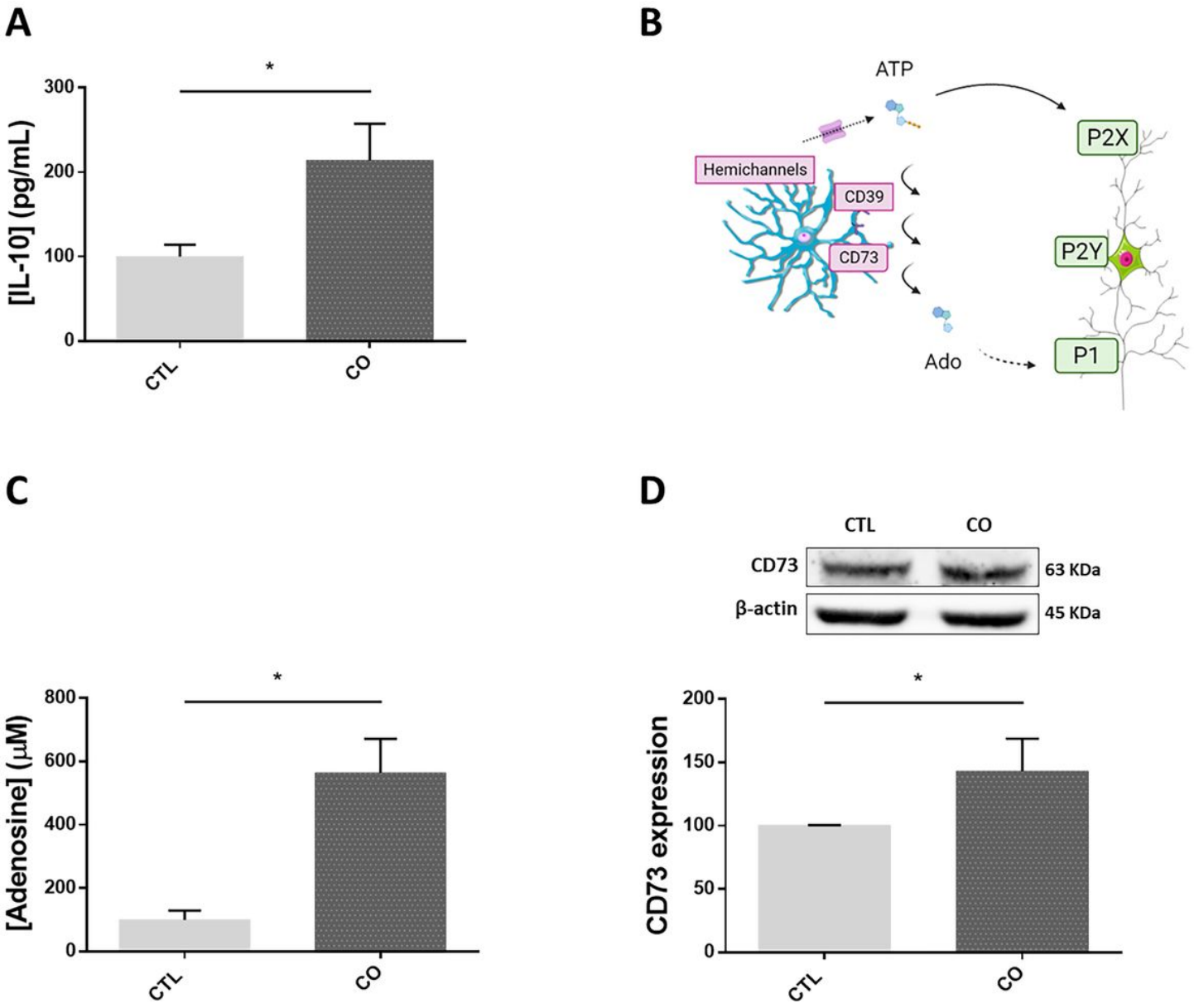

Figure 7

CO stimulates 'resting' microglial secretion of anti-inflammatory factor IL-10 and adenosine. BV2 microglia supernatant was collected, and secretion levels of IL-10 was quantified by ELISA (A). Microglia communicate with neuronal cells via purinergic signaling (B). For the quantification of adenosine in the microglial media, the supernatant was collected, treated and analyzed via HPLC (C). BV2 microglia CD73 protein expression was quantified by Western Blotting (D). CD73 densitometry was normalized for β-actin. Results were normalized to total microglial protein levels. All results are presented as percentage relative to the negative control. n=4-5, error bars represent mean ± SEM, *p<0.05 by one-way ANOVA.

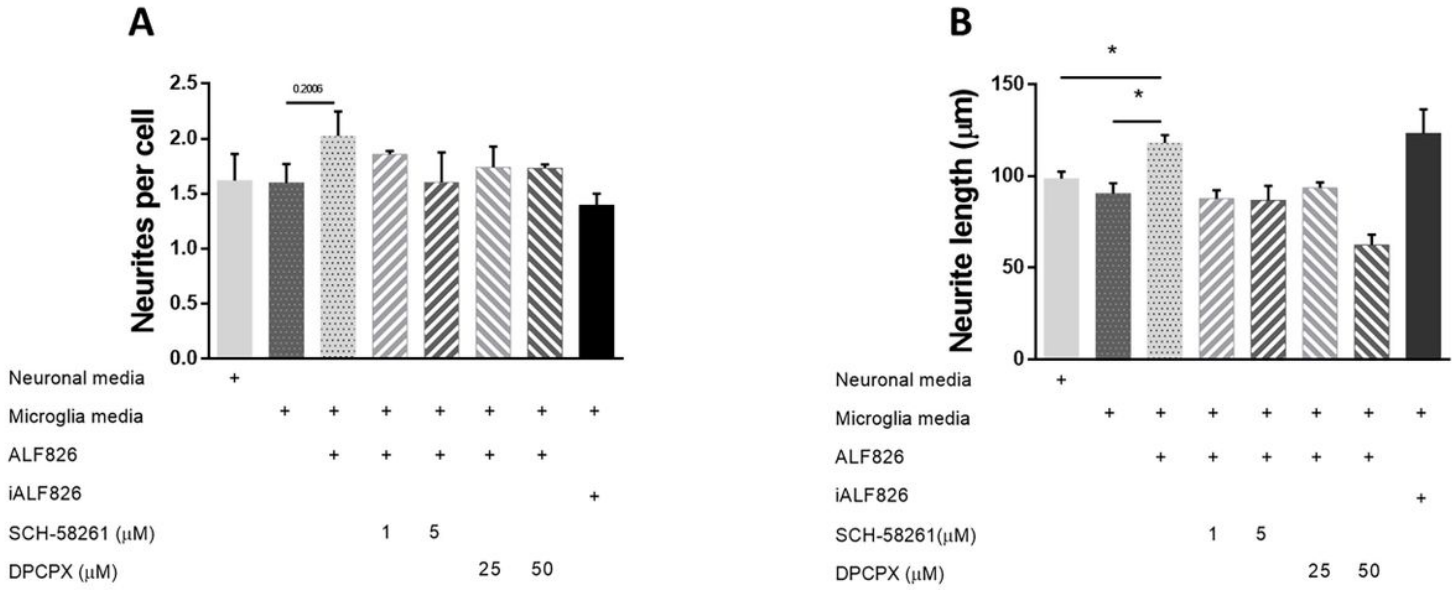

Figure 8

Adenosine receptor blockade reverts neuronal morphological complexity improvement after exposure to CO-treated microglia conditioned medium. CAD neurons treated with BV2 microglia conditioned media and P1 receptor inhibitors (SCH-58261, 1 and 5 μM and DPCPX, 25 and 50 μM) for 24h were labelled with a βIII-tubulin antibody and DAPI, and fluorescence microscopy was performed. Micrographs were analysed and morphological features (A) number of neurites per cell and (B) neurite length were assessed from four independent experiments (15-20 cells per condition). n=4, error bars represent mean ± SEM, *p<0.05 by one-way ANOVA test.

Supplementary Files

This is a list of supplementary files associated with this preprint. Click to download.

- FigS1.tif